J. Fluid Mech. (1968), *vol.* 31, *part* 2, *pp.* 361–377
Printed in Great Britain

Numerical solution of an integral equation for flow from a circular orifice

By BRUCE W. HUNT
The Institute of Hydraulic Research, Iowa City, Iowa†

(Received 28 June 1967)

This study was begun as an attempt to either confirm or disprove conflicting results of previous research upon a classical problem in potential theory. An integral equation resulting from a surface distribution of vorticity is used to solve numerically for the flow through a circular orifice. Free-surface profiles and contraction coefficients are determined for four different ratios of orifice area to pipe area, and a comparison is made between the numerical and experimental results of both this study and previous studies.

1. Introduction

For over a century, potential-flow problems involving free streamlines have given theoretical hydraulicians some of their most rewarding work. Solutions to these problems have been shown to agree closely with experimental measurements in regions where accelerations and velocities of the flow are relatively high, thus permitting practical applications of the mathematical research in this area. However, some of these problems have proved to be so formidable that research workers have been forced to spend their time obtaining numerical approximations rather than solving the problems in closed form. It is no small wonder then that the question of accuracy of these numerical solutions is occasionally raised. The free-surface efflux from an axially symmetric orifice is such a problem.

The first published solution for the axially symmetric jet problem was given by Trefftz (1917). The orifice was assumed to be located in the wall of a reservoir which had boundaries extending to infinity. The problem was formulated in terms of a singular Fredholm integral equation of the second kind, and a technique of trial and error was used to determine the location of the free streamline. Trefftz found the contraction coefficient to be about 0·61, a result which was nearly the same as that obtained by conformal mapping for a two-dimensional slot and which agreed well with an experimental value obtained by Bazin for a round orifice in the bottom of a comparatively large rectangular tank.

A period of over 30 years passed before another solution to the problem was published by Southwell & Vaisey (1948). They used the relaxation method to calculate the flow field for an orifice located in a plate at the end of a finite diameter pipe. The ratio of orifice diameter to pipe diameter was 1:6, and their

† Present address: Department of Civil Engineering, The University of Washington, Seattle, Washington.

computed value of 0·608 for the contraction coefficient agreed almost perfectly with the value of 0·61 obtained by Trefftz (1917) for a pipe of infinitely large diameter.

Later, the relaxation method was applied by Rouse & Abul-Fetouh (1950) to obtain flow characteristics for four different ratios of orifice to pipe diameter. In each case, including the one with an infinite pipe diameter, contraction coefficients were found which differed imperceptibly from those calculated by conformal mapping for the two-dimensional slot. Thus, for all practical purposes, the 40-year-old problem appeared to be completely solved.

Garabedian (1956), however, questioned the accuracy of these previously calculated contraction coefficients. By considering the equation

$$\frac{\partial^2 \psi}{\partial z^2} + \frac{\partial^2 \psi}{\partial r^2} - \frac{\epsilon}{r}\frac{\partial \psi}{\partial r} = 0, \quad \left(\epsilon = \frac{2\delta}{1-\delta}\right), \tag{1.1}$$

where $\psi(r, z, \delta)$ is a stream function, r is the radial co-ordinate, and z is distance along the axis of symmetry, Garabedian obtained a somewhat lower contraction coefficient for the limiting case when the pipe diameter becomes infinitely large. When $\delta = 0$, this equation describes irrotational flow in two dimensions; when $\delta = \frac{1}{3}$, the equation describes axially symmetric irrotational flow. Garabedian was able to show that the ratio of r at infinitely large z to r at the point of separation of the free streamline approached 0 and 1 as δ approached -1 and $+1$, respectively. Since this ratio is calculated to be $\pi/(\pi+2)$ when $\delta = 0$, Garabedian was able to fit a second-degree curve in powers of δ through these three points. Interpolating on this curve then gave the value 0·765 for $\delta = \frac{1}{3}$, which corresponds to a contraction coefficient of 0·586 for the axially symmetric jet. Finally, by utilizing the logarithmic hodograph plane in two dimensions, Garabedian calculated the derivative of r with respect to ϵ when $\delta = \epsilon = 0$. Thus, by using a third-degree polynomial which passed through the three points found previously and which also had the correct slope at $\delta = 0$, Garabedian interpolated for $\delta = \frac{1}{3}$ and arrived at the value of $C_c = 0{\cdot}5793 \doteq 0{\cdot}58$ for the axially symmetric jet.

The intent of the present study was to calculate contraction coefficients by a more refined numerical method for four different ratios of orifice diameter to pipe diameter. Then it was hoped that a comparison between these calculated values, previously calculated values, and experimental values would provide a suitable basis for either confirming or disproving the results of these previous investigations.

2. Dimensional considerations

The radial co-ordinate of the free surface for a liquid jet discharging into the atmosphere should depend upon the following nine variables:

$$r = f(z, r_0, R_0, V_j, \rho, \mu, \gamma, \sigma, k). \tag{2.1}$$

These variables are defined as: r, radial co-ordinate to the free surface; z, distance along the axis of symmetry; r_0, radius of the orifice; R_0, radius of the pipe leading to the orifice; V_j, jet discharge divided by the orifice area; ρ, mass density

of the liquid; μ, dynamic viscosity of the liquid; γ, specific weight of the liquid; σ, surface tension of the liquid; k, scale of surface roughness in the pipe.

Use of the π-theorem to combine these variables into dimensionless groupings yields

$$\frac{r}{r_0} = F_0\left(\frac{z}{r_0}, \frac{r_0}{R_0}, \frac{\rho V_j r_0}{\mu}, \frac{V_j}{(r_0\gamma/\rho)^{\frac{1}{2}}}, \frac{V_j}{(\sigma/\rho r_0)^{\frac{1}{2}}}, \frac{k}{r_0}\right). \tag{2.2}$$

Attention in this study is confined to pipes with smooth surfaces. Thus the last term on the right-hand side of (2.2) will be disregarded, and if the symbols $\boldsymbol{R}$, F and W are used to represent the Reynolds, Froude and Weber numbers, respectively, then (2.2) becomes

$$\frac{r}{r_0} = F_1\left(\frac{z}{r_0}, \frac{r_0}{R_0}, \boldsymbol{R}, F, W\right). \tag{2.3}$$

The contraction coefficient C_c is defined as the ratio of the cross-sectional area of the jet at large z divided by the area of the orifice. This means that C_c is a function of four dimensionless variables, as shown by the following relationship:

$$C_c = F_2\left(\frac{r_0}{R_0}, \boldsymbol{R}, F, W\right). \tag{2.4}$$

Equation (2.4) indicates that the experimental contraction coefficient is a function of the boundary geometry and the relative magnitudes of viscous, gravitational and capillary forces.

The mathematical analysis neglects viscous, gravitational and capillary effects. Hence, for the mathematical results, (2.4) reduces to

$$C_c = F_3(r_0/R_0). \tag{2.5}$$

Equations (2.4) and (2.5) indicate that, in general, the mathematical and experimental contraction coefficients will not coincide. Instead, the mathematical contraction coefficients must be regarded as limiting values of the experimental coefficients, the latter approaching the former when viscous, gravitational, and capillary effects become negligible. There are many published results of experimental investigations concerned with axially symmetric jets, and the findings of four different investigators in the period from 1886 to 1940 (King & Brater 1963; Medaugh & Johnson 1940; Russell 1925) are shown in figure 1 for the case of an orifice in the wall of a large reservoir. These experimental results were not obtained by systematically varying the independent dimensionless variables in (2.4). Thus, it was necessary to plot C_c as a function of the absolute orifice radius r_0 and the ratio r_0/H, where H is the head of water upon the orifice. It is seen from this plot that C_c decreases as r_0/H approaches zero, the decrease in r_0/H representing both a decrease in the effects of gravity and an approach to the same boundary geometry that is assumed in the mathematical model. Also, it is important to note that each one of these investigators has measured values of C_c that are less than the value of 0·61 calculated by Trefftz (1917), Southwell & Vaisey (1948) and Abul-Fetouh (1949) for the irrotational-flow model.

The qualitative result of eliminating capillary, gravitational and viscous effects in the experimental jet can be predicted by physical reasoning. Surface

tension presumably affects the jet in two ways: by causing fluid to cling to the orifice lip and by what Rouse (1961) terms an 'elastic stocking' effect. The clinging or creeping effect probably plays a relatively minor part in determining

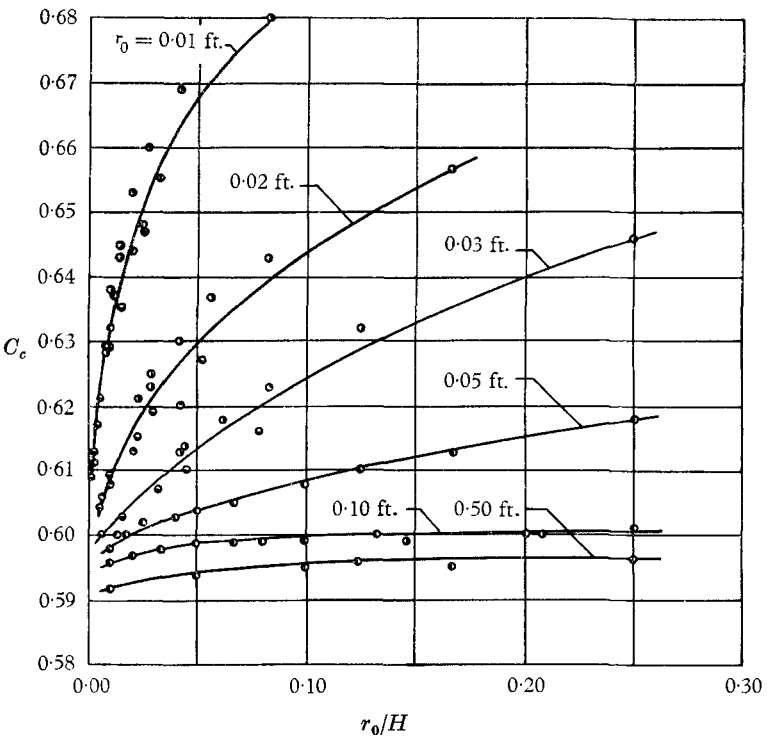

FIGURE 1. Experimental contraction coefficients for an orifice in the wall of a reservoir extending to infinity. ◐, Smith; ◑, Bilton; ◓, Bovey; ◒, Medaugh & Johnson (1940).

C_c, although elimination of this effect could only cause C_c to decrease. Elimination of the 'elastic stocking' effect would cause pressures within the jet to decrease, and the resulting increase in velocity would cause a decrease in the contraction coefficient. Gravity distorts the free-streamline geometry in various ways, depending upon the orientation of the jet with respect to the surface of the earth. For example, a jet directed vertically downward has a smaller contraction coefficient than the same jet would have if directed vertically upward. On the other hand, the free surface of a horizontal jet is distorted by gravity so that its geometric and dynamic characteristics are no longer axially symmetric, and the net result upon C_c in this case is unknown. Viscosity can be expected to affect the jet by altering flow conditions within the boundary layer. As the Reynolds number becomes larger, fluid within the boundary layer is entrained at a faster rate by accelerating flow near the orifice. The end result is that the slope of the 'displaced' boundary (calculated from the boundary-layer displacement thickness) approaches the slope of the actual boundary as viscous effects decrease. Hence, the 'displaced' boundary becomes more nearly perpendicular to the axis of the jet, and the jet is forced to contract more. The final conclusions of this paragraph

may be summarized by saying that elimination of capillary and viscous effects in the experimental jet can only cause a decrease in C_c, while the result of eliminating gravitational effects depends upon the orientation of the jet with respect to the earth's surface.

The conclusions of the preceding paragraph now make it possible to interpret the experimental data shown in figure 1. The influence of gravity upon these contraction coefficients should be very small as r_0/H approaches zero. Therefore, since values of C_c between 0·61 and 0·59 have been measured by four different investigators for small values of r_0/H, and since corrections for capillarity and viscosity could only decrease C_c, it appears that the accuracy of 0·61 for the theoretical contraction coefficient is open to question.

3. Mathematical equations

Line distributions of vorticity have been used by Kochin, Kibel & Rose (1964), Lamb (1932) and Robertson (1965) to generate irrotational velocity fields. However, less use has been made of the fact that surface distributions of vorticity can also generate irrotational velocity fields. These surface distributions lead directly to Fredholm integral equations of the second kind, a fact which forms the basis for the numerical work in this study. Landweber (1951) points out that Vandry (1951) of the Admiralty Research Laboratory in Teddington, England, was one of the first investigators to do pioneer research in this area.

The Biot–Savart law for a line distribution of vorticity is

$$\mathbf{V} = \frac{\Gamma}{4\pi}\int_a^b \frac{d\mathbf{l}\times\mathbf{R}}{R^3}. \tag{3.1}$$

The vector $\mathbf{l}$ is tangent to the line of integration, and the strength Γ of this vortex distribution is constant over the path described by $d\mathbf{l}$. However, if Γ is allowed to vary in a direction normal to $d\mathbf{l}$ so that $\Gamma = \gamma ds$, equation (3.1) may be redefined as the surface integral

$$\mathbf{V} = \int_c^d \frac{\gamma ds}{4\pi}\left(\int_a^b \frac{d\mathbf{l}\times\mathbf{R}}{R^3}\right). \tag{3.2}$$

It is important to realize that in general

$$\mathbf{V} = \mathbf{V}(x_1, x_2, x_3), \quad \gamma = \gamma(t_1, t_2, t_3),$$
$$ds = ds(t_1, t_2, t_3), \quad d\mathbf{l} = d\mathbf{l}(t_1, t_2, t_3),$$
$$\mathbf{R} = (x_1 - t_1)\hat{e}_1 + (x_2 - t_2)\hat{e}_2 + (x_3 - t_3)\hat{e}_3$$
and $$R = |\mathbf{R}| = R(x_1, x_2, x_3, t_1, t_2, t_3).$$

The symbols $\hat{e}_1$, $\hat{e}_2$ and $\hat{e}_3$ denote unit base vectors in the x_1t_1, x_2t_2 and x_3t_3 directions, respectively. The two sets of independent co-ordinates (x_1, x_2, x_3) and (t_1, t_2, t_3) are often considered to be co-ordinates of the two points $p(x_1, x_2, x_3)$ and $q(t_1, t_2, t_3)$ in space. Hence, the subscripts p and q will be used to show that a variable is a function of the 'fixed' point co-ordinates (x_1, x_2, x_3) and the 'variable' point co-ordinates (t_1, t_2, t_3), respectively. This notation allows (3.2) to be written in the following form:

$$\mathbf{V}_p = \int_c^d \frac{\gamma_q ds_q}{4\pi}\left(\int_a^b \frac{d\mathbf{l}_q\times\mathbf{R}_{pq}}{R_{pq}^3}\right). \tag{3.3}$$

If the region of interest **V** is interior to its boundary surface S, then, when point p lies upon S, it is possible to deduce the following equation from (3.3):

$$V_{p-} = \hat{T}_p \cdot \int \frac{\gamma_q dS_q}{4\pi} \left(\int_S \frac{d\mathbf{l}_q \times \mathbf{R}_{pq}}{R_{pq}^3} \right) + \frac{\gamma_p}{2}. \tag{3.4}$$

The unit vector $\hat{T}_p$ is in the direction of flow and tangent to S at point p. The function γ_p is found to be

$$\gamma_p = V_{p-} - V_{p+}, \tag{3.5}$$

where V_{p-} and V_{p+} are scalar magnitudes of the vector velocity **V** on the interior and exterior sides, respectively, of S. For the interior problem under consideration, the velocity V_{p+} vanishes. If the velocity V_{p-} is denoted by U, substitution of (3.5) into (3.4) then gives an integral equation for the interior problem:

$$\frac{U_p}{2} = \hat{T}_p \cdot \int \frac{U_q ds_q}{4\pi} \left(\int_S \frac{d\mathbf{l}_q \times \mathbf{R}_{pq}}{R_{pq}^3} \right). \tag{3.6}$$

The theory of Fredholm states that (3.6) has no solution unless the characteristic value of this equation is unity, in which case there are a finite number of independent, nontrivial solutions for U. Since a unique solution to this problem is known to exist physically, it can be concluded that unity is an eigenvalue of (3.6) of multiplicity one, and one and only one solution U exists. It will be shown in the next section, however, the (3.6) can be approximated by an inhomogeneous integral equation of the second kind simply by specifying U on a portion of S. In that case, a unique solution exists if unity is not an eigenvalue of the approximate inhomogeneous equation.

A simple argument can be used now to show that the velocity $U(x_1, x_2, x_3)$ must be zero in the entire region exterior to S. This conclusion is based upon the fact that the velocity V_{p+} on the exterior side of S vanishes. Since irrotational motion is impossible in a region where the total velocity vanishes on the boundary S, then the velocity must vanish everywhere within the region.

4. Formulation of the problem

There is a boundary condition which must be imposed at the free surface in order to fix a location of the free streamline. This is the condition of constant velocity upon the free surface, obtained from the Bernoulli equation by considering the head upon the orifice to be so large that the gravity term may be neglected. A method of trial and error was used in this study to find a free streamline which conformed to this boundary condition. A geometry for the free streamline was assumed initially, and then velocities at various points along the free surface were calculated and checked for the constant-velocity condition. Finally, the position and shape of the free streamline were corrected accordingly, and the process was repeated.

If an exact mathematical solution to this problem were available, it would show that the free streamline only reaches its asymptotic radius r_a at a cross-section infinitely far downstream from the orifice. The solution would also show that flow within the pipe is fully uniform only at a cross-section infinitely far upstream from the orifice. For the approximate numerical solution of this problem, however, it was assumed that the asymptotic radius of the free streamline was reached in a distance of about 1·6 orifice diameters downstream from the orifice, and that

uniform flow was present in the pipe about 1·5 pipe diameters upstream from the orifice. Inspection of the results of Abul-Fetouh's investigation shows clearly that these are very reasonable assumptions. Once these two approximations are

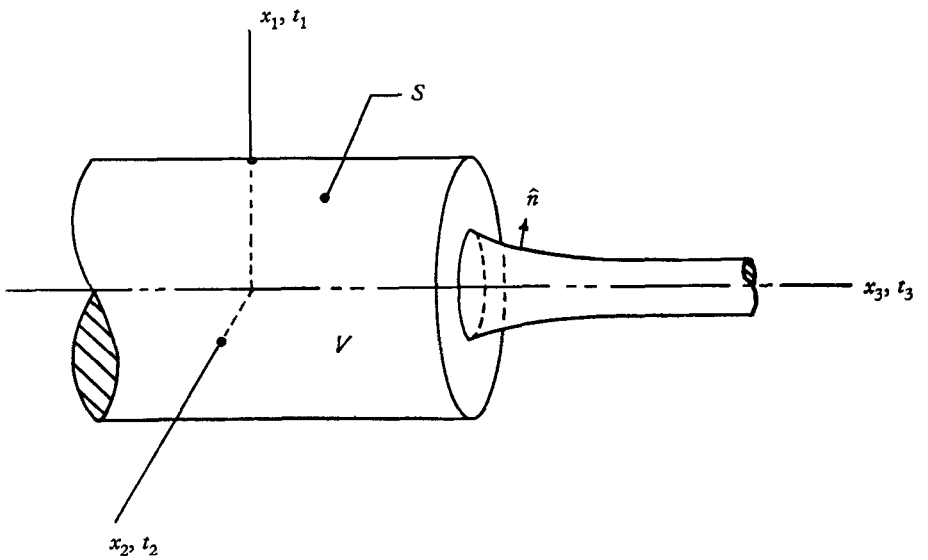

FIGURE 2. Flow through an orifice located in a plate at the end of a pipe.

introduced, (3.6) can be put in the form of an inhomogeneous integral equation of the second kind,

$$\frac{U_p}{2} = \hat{T}_p \cdot \int \frac{U_q dS_q}{4\pi} \left(\int_{S_{0a}} \frac{d\mathbf{l}_q \times \mathbf{R}_{pq}}{R_{pq}^3} \right) + f(x_1, x_2, x_3), \tag{4.1}$$

where $$f(x_1, x_2, x_3) = U_{+\infty} \left[\hat{T}_p \cdot \int \frac{ds_q}{4} \left(\int_{S_{a+\infty}} \frac{d\mathbf{l}_q \times \mathbf{R}_{pq}}{R_{pq}^3} \right) + \left(\frac{r_a}{R_0} \right)^2 \hat{T}_p \cdot \int \frac{ds_q}{4\pi} \left(\int_{S_{-\infty 0}} \frac{d\mathbf{l}_q \times \mathbf{R}_{pq}}{R_{pq}^3} \right) \right]. \tag{4.2}$$

The symbols $S_{-\infty a}$, S_{0a} and $S_{a+\infty}$ denote portions of the surface S for

$$-\infty < x_3 < 0, \quad 0 \leqslant x_3 \leqslant a \quad \text{and} \quad a < x_3 < +\infty,$$

respectively, $U_{+\infty}$ is the asymptotic free-surface velocity, the point $x_3 = a$ is where the asymptotic radius r_a was assumed to be reached, and R_0, as defined previously, is the pipe radius. The point $x_3 = 0$ is located on the axis of symmetry where uniform flow was assumed to start in the pipe.

5. Numerical treatment of the integral equation

The cylindrical symmetry present in the orifice problem made it most convenient to switch from Cartesian to cylindrical co-ordinates. Therefore, after restricting point $p(x_1, x_2, x_3)$ to the (x_1, x_2)-plane, the following change of co-ordinates was made:

$$x_1 = r, \qquad x_2 = 0, \qquad x_3 = z,$$
$$t_1 = \rho \cos\theta, \quad t_2 = \rho \sin\theta, \quad t_3 = \zeta.$$

The x_1, x_2, x_3 and t_1, t_2, t_3 co-ordinate axes were made to coincide as shown in figure 2, and the angular displacement θ was measured from the (x_1, t_1)-axis

toward the (x_2, t_2)-axis in the sense of a right-handed co-ordinate system. Thus, $d\mathbf{l}_q = \rho d\theta\hat{\theta}$ and $(ds_q)^2 = (d\rho)^2 + (d\zeta)^2$, where $\hat{\theta}$ is a unit base vector in the θ direction for the ρ, θ, ζ system. Once these substitutions were made in (4.1) and (4.2), it was possible to multiply through by 4π and integrate with respect to θ to obtain

$$2\pi U_p - \int_{s_q(\zeta_0)}^{s_q(\zeta_a)} U_q K(r,z,\rho,\zeta)\,ds_q = U_{+\infty}\left[\int_{s_q(\zeta_a)}^{s_q(+\infty)} K(r,z,\rho,\zeta)\,ds_q + \left(\frac{r_a}{R_0}\right)^2 \int_{s_q(-\infty)}^{s_q(\zeta_0)} K(r,z,\rho,\zeta)\,ds_q\right], \tag{5.1}$$

where the kernel function $K(r,z,\rho,\zeta)$ is

$$K(r,z,\rho,\zeta) = \frac{4\rho}{[(r+\rho)^2+(z-\zeta)^2]^{\frac{3}{2}}}\left\{\left[\left(\rho+r-\frac{2r}{k^2}\right)\cos B_p + \left(\frac{2}{k^2}-1\right)(z-\zeta)\sin B_p\right] \times \frac{E(k,\frac{1}{2}\pi)}{(1-k^2)} + 2[r\cos B_p - (z-\zeta)\sin B_p]\frac{F(k,\frac{1}{2}\pi)}{k^2}\right\}. \tag{5.2}$$

The symbols $F(k,\frac{1}{2}\pi)$ and $E(k,\frac{1}{2}\pi)$ represent complete elliptic integrals of the first and second kind, respectively, the angle B_p is defined as

$$B_p = \tan^{-1}(dr/dz)$$

evaluated at the point $p(r,0,z)$, and the elliptic modulus k is defined by

$$k^2 = \frac{4r\rho}{(r+\rho)^2+(z-\zeta)^2} \quad (0 < k^2 \leqslant 1). \tag{5.3}$$

Details of this integration are given by Hunt (1967). Careful examination of (5.2) discloses the fact that $K(r,z,\rho,\zeta) \to +\infty$ as the points p and q approach each other along the arc s (s is the line formed by the intersection of the half plane $\theta = 0$ and the surface S). It is shown also by Hunt (1967) that

$$\lim_{q\to p} K(r,z,\rho,\zeta) = \frac{\cos B_p}{r}[\ln(r8) - 1] + \frac{dB_p}{ds_p} - \lim_{s_{pq}\to 0}\left[\frac{\cos B_p}{r}\ln|s_{pq}|\right], \tag{5.4}$$

where $s_{pq} = s_q - s_p$ is arc length measured from point p to point q. Thus, even though $K(r,z,\rho,\zeta) \to +\infty$ as $q \to p$ along s, the integral

$$\int_{s_q(\zeta_0)}^{s_q(\zeta_a)} U_q K(r,z,\rho,\zeta)\,ds_q$$

in (5.1) quite definitely exists.

Numerical solution of (5.1) was accomplished by dividing the arc length s from $\zeta = \zeta_0$ to $\zeta = \zeta_a$ into N segments and rewriting (5.1) in the approximate form

$$2\pi U_p - \sum_{i=1}^{N} U_i \int_{s_{i-1}}^{s_i} K(r,z,\rho,\zeta)\,ds_q = U_{+\infty}\left[\int_{s_q(\zeta_a)}^{s_q(+\infty)} K(r,z,\rho,\zeta)\,ds_q + \left(\frac{r_a}{R_0}\right)^2 \int_{s_q(-\infty)}^{s_q(\zeta_0)} K(r,z,\rho,\zeta)\,ds_q,\right] \tag{5.5}$$

where U_i is a mean value of U_q that is assumed to occur halfway between s_{i-1} and s_i. This approximation, according to Kantorovich & Krylov (1958), is

known as the method of Krylov & Bogoliubov. The length of the segments from s_{i-1} to s_i varied from relatively large values in regions of nearly uniform flow to about $r_0/32$ in regions of rapid acceleration close to the orifice and the point of stagnation. The number N was taken to be about 60. After each segment from s_{i-1} to s_i was split in half, evaluation of the N integrals was accomplished using Simpson's rule. A system of N equations for the N unknowns U_i was obtained by choosing point p to be at the midpoint of each of the N arc-length segments. Solution of these equations was accomplished with an IBM-7044 computer at the University of Iowa, and solution time for a given geometry of the free streamline was approximately three minutes.

When integrating over the segment of arc which contained point p, the following method, suggested by Landweber, was used to 'remove' the singularity. The integral from s_{p-1} to s_p was replaced by

$$U_p \int_{s_{p-1}}^{s_p} K(r,z,\rho,\zeta)\,ds_q = U_p \int_{s_{p-1}}^{s_p} \left[K(r,z,\rho,\zeta) + \frac{\cos B_p}{r} \ln|s_{pq}|\right] ds_q - U_p \frac{\cos B_p}{r} \int_{s_{p-1}}^{s_p} \ln|s_{pq}|\,ds_q. \tag{5.6}$$

The first integral on the right-hand side of (5.6) can be evaluated by Simpson's rule, since (5.4) clearly shows that the singularity has been 'subtracted out'. The second integral can be integrated exactly.

Evaluation of both integrals on the right-hand side of (5.5) was fairly straightforward, since no singularity appears in their integrand. The substitution $\pm(s+s_0) = \tan\phi$ changes the lower and upper limits of integration to $\phi = \phi_0 > 0$ and $\phi = +\frac{1}{2}\pi$, respectively, and the resulting integrals were evaluated using Simpson's rule with 40 equally spaced increments of ϕ.

One of the most critical steps in the numerical solution was determining slopes and curvatures along the free streamline at the midpoint of each of the intervals from s_{i-1} to s_i. Since each interval was small enough to allow the enclosed arc length to be approximated by the length of a straight line joining the end-points, it was decided to use the slope of each of these straight-line segments for the slope at the midpoint of each arc. Once slopes were found at numerous points along the free streamline, it was possible to represent the slope in a piecewise manner as a function of z by

$$\tan B = f_1(z), \tag{5.7}$$

where $f_1(z)$ is a second-degree polynomial passing through three successive points. Differentiating (5.7) with respect to s then allowed the curvature to be calculated at the midpoint by the formula

$$\frac{dB}{ds} = \frac{df_1(z)/dz}{[1+f_1^2(z)]^{\frac{3}{2}}}. \tag{5.8}$$

Obviously, (5.8) cannot be used in a region close to the orifice, since the slope (and apparently the curvature too) becomes infinite at the point of separation. In this region, since $\cot B = 0$ at the point of separation, it was found more convenient to replace (5.7) by

$$\cot B = f_2(z) \tag{5.9}$$

and calculate curvatures near the point of separation by the formula

$$\frac{dB}{ds} = -\frac{|f_2(z)|(df_2(z)/dz)}{[1+f_2^2(z)]^{\frac{3}{2}}}, \tag{5.10}$$

which may be obtained from (5.9) simply by differentiating with respect to s.

Details of the method used for locating the free streamline consisted of initially

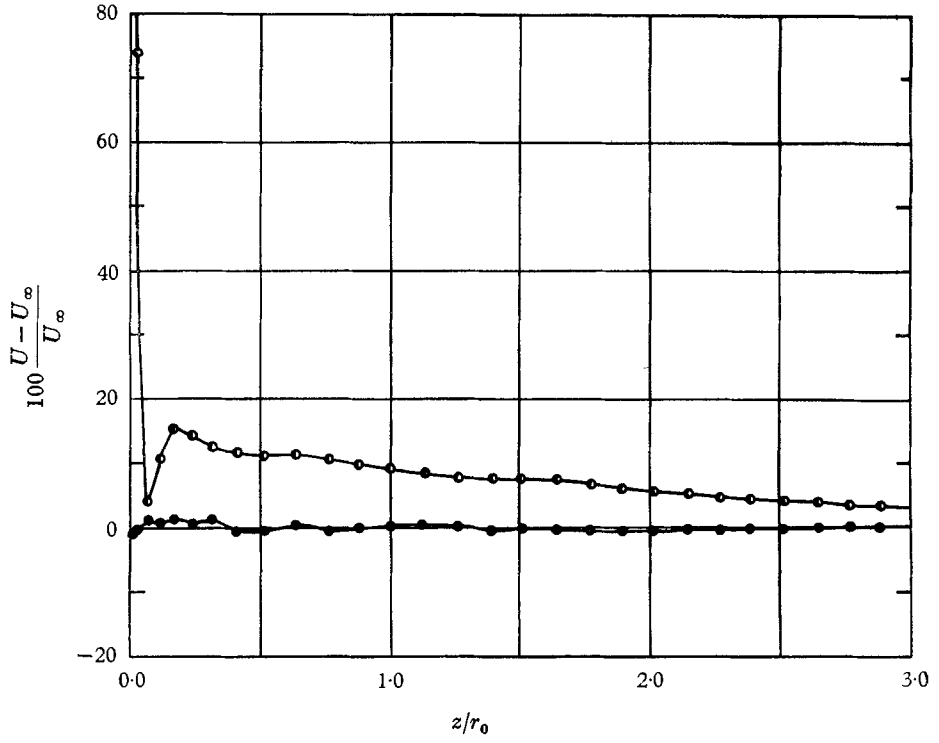

FIGURE 3. Percentage variation from the constant-velocity condition for the two theoretical profiles shown in figure 5. ◐, Abul-Fetouh (1949); ●, Hunt (1967).

choosing an asymptotic radius r_a. Next, the shape of the free streamline between the orifice and the region of uniform flow was adjusted by trial and error until velocities along the portion of the free surface farthest from the orifice were essentially constant. Finally, if free-surface velocities in the vicinity of the orifice were higher than the chosen asymptotic velocity, the asymptotic radius was decreased. Conversely, if velocities in this region were too low, the asymptotic radius was increased. The entire process had to be repeated a number of times until a satisfactory free-streamline geometry was found. This usually meant calculating velocities along the free surface for ten to twenty different geometries in order to obtain one solution.

Calculations were stopped when a geometry for the free steamline was found which satisfied the constant-velocity condition within $\pm 1{\cdot}5\%$ of the asymptotic velocity. Velocities along the free surface were extremely sensitive to very small changes in form and position of the free streamline. This was particularly true close to the orifice. An indication of this sensitivity is given in figure 3, where per

cent deviaton from the constant-velocity condition is shown for the two theoretical profiles plotted in figure 5. The radii for these two profiles do not differ from each other by more than 3% at any point. However, deviations from the asymptotic velocity range from about 3% to 108% for the one profile, while the other profile satisfies the $\pm 1{\cdot}5\%$-error criterion used for this study.

6. Experimental measurements

There is a wealth of published experimental data concerning contraction coefficients and discharge coefficients for axially symmetric jets, but relatively little experimental work has been concerned with measuring entire surface profiles. For that reason, it was decided to measure experimentally under very special conditions the free-surface profile for one of the four boundary geometries considered in this study.

Since the purpose of this experimental work was to detect extremely small differences between the experimental and calculated surface profiles (differences of $r/r_0 \doteq 0{\cdot}025$), it was necessary to use great precision in taking measurements. Furthermore, in order to make the comparison as meaningful as possible, the effects of gravity, viscosity, and surface tension, had to be minimized. As shown previously, this meant making the Froude, Reynolds and Weber numbers as large as possible. It also meant that flow separation along the boundary was undesirable, and thus it was decided to use a large orifice located in the wall of a relatively large tank.

Experimental measurements were made using a jet which discharged vertically downward through a 2 in. radius orifice in the bottom of a large rectangular steel tank. This tank, which ordinarily served as a constant-head tank for other experimental work at the Iowa Institute of Hydraulic Research, is 14 ft. wide, 24 ft. long, and 6 ft. 5 in. deep. The distance from the centre of the orifice to the only obstruction on the otherwise smooth floor of the tank was about 3 ft. This obstruction was a 3 in. angle iron, and its influence upon the flow was considered negligible, since velocities in this region were calculated to be about 0·1% of the free-streamline velocity at the orifice. The orifice itself was cut in a piece of stainless steel so that the edge of the orifice could be ground to a thickness of about 0·004 in., and this $5\frac{1}{2}$-inch diameter stainless-steel insert was set into the bottom of the tank so that its wetted surface was flush with the interior tank surface.

Radial measurements of the free surface were made by using two sharp brass prongs which converged upon opposite sides of the jet at the same time. Distance between the two prong points was read from an attached micrometer scale to one thousandth of an inch, and this reading was divided in half to obtain the jet radius. A point gauge was rigidly fastened to the bottom of the tank so that its longitudinal axis was vertical and parallel to the longitudinal axis of the jet. The caliper was mounted upon the end of a second point gauge, which crossed the vertical point-gauge at right angles. These two point-gauges were joined together in a way that allowed the caliper to be moved in both the horizontal and vertical directions. The distance of the caliper prong points from the orifice plate was measured with the vertical point-gauge to one thousandth of a foot.

Since measurements were made on a vertical jet, it was a simple matter to apply an approximate gravitational correction to the measured profile. If the free surface below the orifice were unaffected by gravity, the constant velocity along the free streamline for a head H on the orifice would be

$$V = (2gH)^{\frac{1}{2}}.$$

The actual experimental velocity at a point on the free streamline is approximately

$$V = [2g(H+z)]^{\frac{1}{2}},$$

where z is distance below the orifice. Requiring flow rates to be the same for these two cases then gives for the corrected radius r_c

$$r_c \doteq r\left(1+\frac{z}{H}\right)^{\frac{1}{4}} \geqslant r. \tag{6.1}$$

The experimental procedure consisted of filling the tank to its top, removing a cap over the orifice, and taking measurements for 15 min, in the course of which the water level in the tank dropped approximately 2 ft. Then the tank was filled again and the procedure was repeated several times to obtain the remaining measurements. This method was adopted in preference to the alternative method of keeping a constant head upon the orifice, because it was found that flow from the pumps disturbed the free surface of the jet. When the pumps were not running, the upper portion of the free surface appeared glass-smooth and perfectly steady. However, this smoothness and steadiness gradually lessened with increasing distance from the orifice, and it was considered impossible to make accurate measurements for $z/r_0 > 1{\cdot}5$.

7. Discussion of the results

The contraction coefficients calculated in this study by (5.5) were

$$0{\cdot}5776 \doteq 0{\cdot}578, \quad 0{\cdot}5938 \doteq 0{\cdot}594, \quad 0{\cdot}6241 \doteq 0{\cdot}624 \quad \text{and} \quad 0{\cdot}6908 \doteq 0{\cdot}691$$

for orifice-to-pipe area ratios of 0·00, 0·25, 0·50 and 0·75, respectively. These results are plotted in figure 4 along with the values calculated by Abul-Fetouh (1949) and some experimental values determined by Weisbach (1855). The value 0·578 for the limiting case of an infinite pipe diameter agrees closely with Garabedian's (1956) value of 0·579, and contraction coefficients for the other three cases are also lower than corresponding values calculated by Abul-Fetouh. Close examination of figure 4 discloses the interesting paradox that experimental magnitudes of the contraction coefficients seem to agree more closely with Abul-Fetouh's theoretical curve, while the shape of the experimental curve appears to agree more nearly with the shape of the theoretical curve determined in this study.

The mathematically computed free surface for the orifice-to-pipe area ratio of 0·00 is shown in figure 5. Points determined experimentally are also plotted in figure 5 for comparison with the corresponding theoretical profiles calculated in both this work and in the work by Abul-Fetouh. All of these experimental points have been approximately corrected for gravitational effects with (6·1). The closeness of the corrected experimental points determined in runs 1 and 2 is

evidence of the sensitivity of the experimental measurements. Of utmost importance is the fact that this experimental profile, after being corrected for gravitational effects, has an asymptotic radius which is less than Abul-Fetouh's

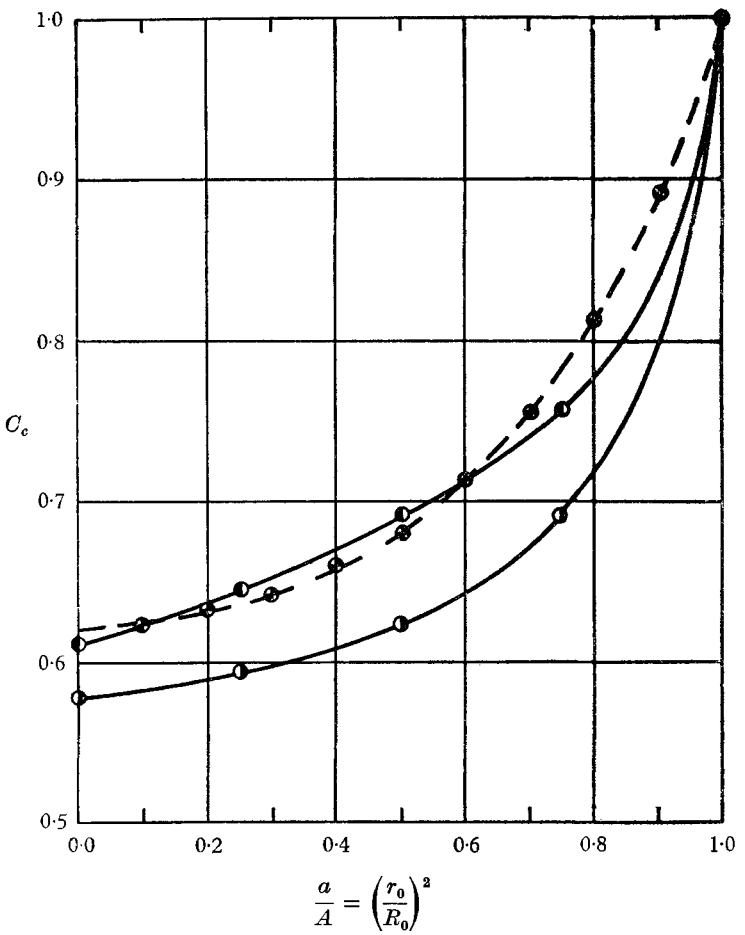

FIGURE 4. Contraction coefficients for different ratios of orifice area to pipe area. ◐, Abul-Fetouh (1949), theoretical; ⊛, Weisbach (1855), experimental; ◑, Hunt (1967), theoretical.

theoretical asymptotic radius but greater than the theoretical asymptotic radius found in this study. It was shown in a previous section that a reduction in viscous and capillary effects could only cause the asymptotic radius to decrease. Since the mathematical analysis neglects the effects of viscosity and capillarity, then the only logical conclusion is that the potential-flow profile must have a smaller asymptotic radius than the corrected experimental profile shown in figure 5. Therefore, there is certainly reason to believe that, when $a/A = 0$, the value of 0·58 is very close to the exact mathemetical contraction coefficient.

Since much of this study is concerned with the mathematical aspects of the problem, it seems fitting to close the discussion with a review of some of the

weaknesses of various methods that have been used to obtain numerical solutions. All of these methods have certain failings.

Trefftz's original attack on the problem in 1916, using integral equations, was a significant step forward in a relatively unexplored direction. However, there are

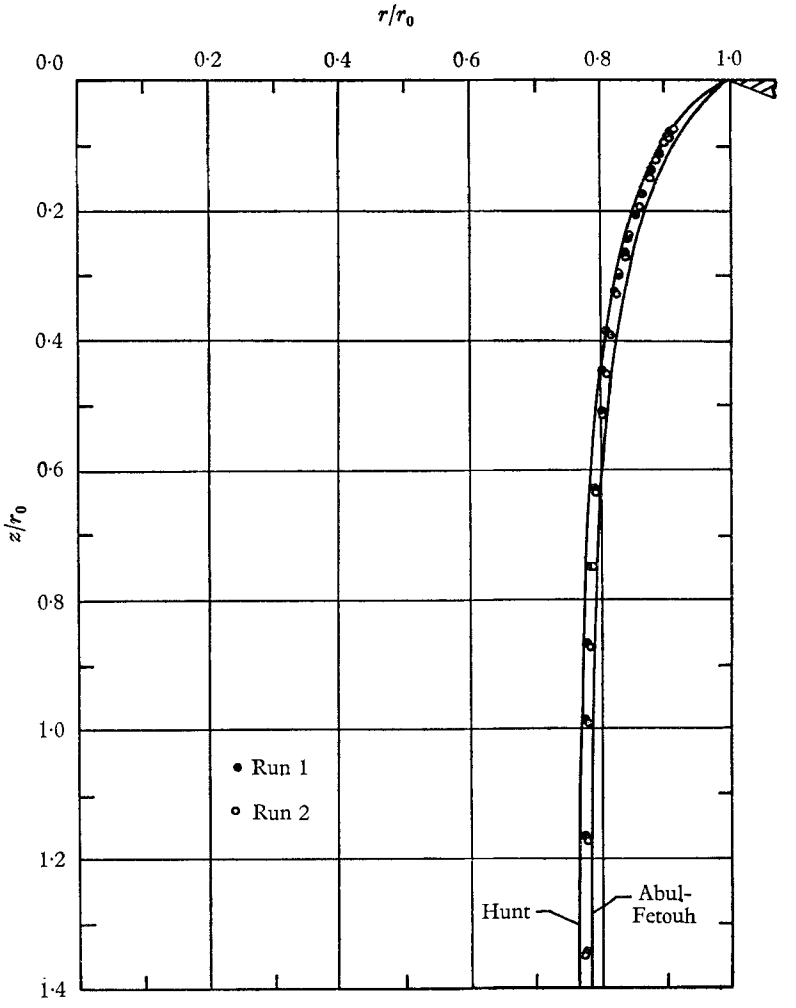

FIGURE 5. Free-surface profiles for an orifice in the wall of a reservoir extending to infinity.

at least two serious criticisms which can be made about his method. First, instead of comparing velocities along the free streamline, Trefftz compared values of the flow potential as a check on the constant-velocity condition. Even if the assumed and calculated values of the flow potential coincide at a finite number of points along the free surface, it does not follow that derivatives of the potential must coincide at these points, too. Secondly, Trefftz used only six points along the free streamline, and these are hardly enough points to include the all-important effects of highly curvilinear flow near the orifice.

The relaxation or finite-difference approach used by Southwell & Vaisey (1948) and by Abul-Fetouh (1949) is undoubtedly just as accurate as the method of integral equations—provided that the intervals between the mesh points are chosen sufficiently small. Gilbarg (1960) feels that one possible source of inaccuracy in finite-difference methods is truncation error in a region near the point of separation. He cites one example given in a governmental report in which velocities computed by relaxation along a free streamline for a plane-flow problem were all within $\pm 0{\cdot}7\,\%$ of each other, yet an exact solution to this problem showed that exact and calculated values of the free-surface ordinate differed by as much as $10\,\%$. One other criticism not mentioned by Gilbarg is the difficulty of evaluating at the free surface partial derivatives of the stream function in the vertical and horizontal directions. These derivatives must be used to check the constant-velocity condition. Abul-Fetouh determined derivatives by differentiating a second-degree polynomial which passed through three points. Then he evaluated derivates at the end-point—a procedure which can be extremely risky. Southwell & Vaisey's method was no better in this respect.

Garabedian's method depends upon interpolating a numerical value from a third-degree polynomial which satisfies four given conditions. As mentioned previously, passing an Nth-degree polynomial through $N+1$ points on another curve does not mean in general that the two curves will coincide. This is simply because slopes and higher derivatives may be different at these $N+1$ points. However, to Garabedian's credit, his third-degree polynomial was determined so that it passed through a point with the correct slope close to where his final value was interpolated. A more detailed criticism concerning possible errors of this type in Garabedian's solution is given in a discussion by Landweber (1962).

Two weaknesses of the integral-equation approach used in this study are the approximation made in (5.5) and the need for accurate values of free-streamline curvature near the point of separation. An estimate of the error involved by solving (5.5) as an approximation to (5.1) is given by Kantorovich & Krylov (1958), but it is impossible to use formulas given in this reference because of the singularity present in the kernel function $K(r, z, \rho, \zeta)$. In defence of this approximation, however, it should be noted that the spacings s_{i-1} to s_i along the boundary were chosen in a way calculated to minimize errors in the approximation. Also, when point q is on the actual free streamline, U_q is a constant and (5.5) is truly exact. Probably more important for the question of accuracy are values of curvature found near the point of separation. Numerical calculations made with (5.10) gave curvatures which were relatively high near the orifice, and if the two-dimensional flow is any indication of the behaviour of axially symmetric flow in this region, then the curvature becomes infinite at the point of separation. Use of smaller curvatures in this region was found to increase the asymptotic radius of the jet without seriously affecting the shape of the free streamline.

8. Conclusions

The results of this study allow the following general conclusions to be made.

Free-streamline problems in fluid mechanics may be solved more efficiently with integral equations derived from surface-vortex distributions than with

either relaxation techniques or integral equations derived from source-and-sink distributions. This is because unknown velocities on the boundary are obtained directly without having to differentiate a potential function or solve for unknowns within the flow field itself.

Boundary velocities calculated from these integral equations are extremely sensitive to small changes in position, slope and curvature of the boundary. This means that ordinates, slopes and curvatures of the boundaries must be known very accurately in order to achieve a corresponding high degree of accuracy in numerical solutions.

Numerically calculated and experimentally obtained free-surface profiles for the axially symmetric jet appear to check closely when the Froude, Reynolds and Weber numbers are all relatively large. It is only when contraction coefficients computed from the squares of corresponding radii are compared that differences become appreciable.

Numerical and experimental results presented in this study indicate that mathematically determined contraction coefficients for axially symmetric jets are slightly less in magnitude than contraction coefficients calculated mathematically for the corresponding two-dimensional jets.

The writer would like to thank Dean Hunter Rouse and Dr Louis Landweber for advising him on the physical and theoretical aspects of the problem, respectively. The study was initially suggested by Dean Rouse.

REFERENCES

ABUL-FETOUH, A. 1949 Characteristics of irrotational flow from axially symmetric orifices. Ph.D. Dissertation, University of Iowa, Iowa.

GARABEDIAN, P. 1956 Calculation of axially symmetric cavities and jets. *Pacif. J. Math.* **6**, 611–84.

GILBARG, D. 1960 Jets and Cavities. *Encyclopedia of Physics*, **9**, 311–445.

HUNT, B. 1967 Numerical solution of an integral equation for flow from a circular orifice. Ph.D. Dissertation, University of Iowa, Iowa.

KANTOROVICH, L. & KRYLOV, V. 1958 *Approximate Methods of Higher Analysis.* Groningen: P. Noordhoff Ltd.

KING, H. & BRATER, E. 1963 *Handbook of Hydraulics.* New York: McGraw-Hill.

KOCHIN, N., KIBEL, I. & ROSE, N. 1964 *Theoretical Hydromechanics.* New York: Interscience Publishers.

LAMB, H. 1932 *Hydrodynamics.* New York: Dover Publications.

LANDWEBER, L. 1951 The axially symmetric potential flow about elongated bodies of revolution. *David Taylor Model Basin Rept.* no. 761, NS 715-084.

LANDWEBER, L. 1962 Calculation of potential flows with free streamlines (discussion). *ASCE J. of the Hydraulics Division*, **88**, 223.

MEDAUGH, F. & JOHNSON, G. 1940 Investigations of the discharge and coefficients of small circular orifices. *Civil Engineering*, **10**, 422–4.

ROBERTSON, J. 1965 *Hydrodynamics in Theory and Application.* Englewood Cliffs: Prentice-Hall.

ROUSE, H. 1946 *Elementary Mechanics of Fluids.* New York: John Wiley and Sons.

ROUSE, H. (Editor) 1959 *Advanced Mechanics of Fluids.* New York: John Wiley and Sons.

ROUSE, H. 1961 *Fluid Mechanics for Hydraulic Engineers*. New York: Dover Publications.

ROUSE, H. & ABUL-FETOUH, A. 1950 Characteristics of irrotational flow through axially symmetric orifices. *J. Appl. Mech.* **17**, no. 4, 421–6.

RUSSELL, G. 1925 *Text-book on Hydraulics*. New York: Henry Holt and Co.

SOUTHWELL, R. & VAISY, G. 1948 Relaxation methods applied to engineering problems. XII. Fluid motions characterized by free stream lines. *Phil. Trans. Roy. Soc. Lond.* A, **240**, 117–61.

TREFFTZ, E. 1917 Über die Kontraktion kreisförmiger Flussigkeitsstrahlen. *Z. Math. Phys.* **64**, 34.

VANDRY, F. 1951 A direct iteration method for the calculation of the velocity distribution of bodies of revolution and symmetrical profiles. *Admiralty Research Laboratory Rept.* R 1/G/HY/12/2.

WEISBACH, J. 1855 *Die Experimental-Hydraulik*. Freiberg: J. S. Englehardt.